

Supporting Information

for

Rational design of a lysosome-targeting and near-infrared absorbing Ru(II)-BODIPY conjugate for photodynamic therapy

Liping Qiao,^a Jiangping Liu,^{*a} Yunhong Han,^a Fangmian Wei,^a Xinxing Liao,^a Cheng Zhang,^a Lina Xie,^a Liangnian Ji,^a and Hui Chao^{*a,b}

^a MOE Key Laboratory of Bioinorganic and Synthetic Chemistry, School of Chemistry, Sun Yat-Sen University, Guangzhou 510275, P. R. China.

^b MOE Key Laboratory of Theoretical Organic Chemistry and Functional Molecule, School of Chemistry and Chemical Engineering, Hunan University of Science and Technology, Xiangtan, 400201, P. R. China.

Email: cesliujiangping@foxmail.com, ceschh@mail.sysu.edu.cn

Table of Contents

| | |
|--|---|
| Experimental Section | 1 |
| Materials and instrumentation..... | 1 |
| Synthesis and characterization..... | 2 |
| Electron paramagnetic resonance (EPR) assay | 3 |
| ¹ O ₂ quantum yield measurement..... | 4 |
| Log <i>P</i> _{O/W} measurement | 4 |
| Cell line and culture conditions | 5 |
| Cellular uptake assay | 5 |
| Cellular uptake mechanism study | 5 |
| Intracellular localization | 6 |
| Intracellular ROS generation | 6 |
| Lysosomal membrane permeabilization analysis..... | 6 |
| Detection of cathepsin B release..... | 7 |
| Caspase-3/7 activity assay | 7 |
| Annexin V-FITC/PI staining assay | 7 |

| | |
|--|----|
| In vitro cell viability test (MTT assay) | 7 |
| In vivo fluorescence imaging experiment | 8 |
| NIR PDT in vivo..... | 8 |
| Supporting Figures | 10 |
| Fig. S1..... | 10 |
| Fig. S2..... | 11 |
| Fig. S3..... | 12 |
| Fig. S4..... | 13 |
| Fig. S5..... | 14 |
| Fig. S6..... | 14 |
| Fig. S7..... | 15 |
| Fig. S8..... | 15 |
| Fig. S9..... | 16 |
| Fig. S10..... | 16 |
| Fig. S11..... | 17 |
| Fig. S12..... | 17 |
| Fig. S13..... | 18 |
| Fig. S14..... | 18 |
| Fig. S15..... | 19 |
| Fig. S16..... | 19 |
| Fig. S17..... | 20 |
| Supporting Tables | 21 |
| Table S1..... | 21 |
| Table S2..... | 21 |
| References | 22 |

Experimental Section

Materials and instrumentation

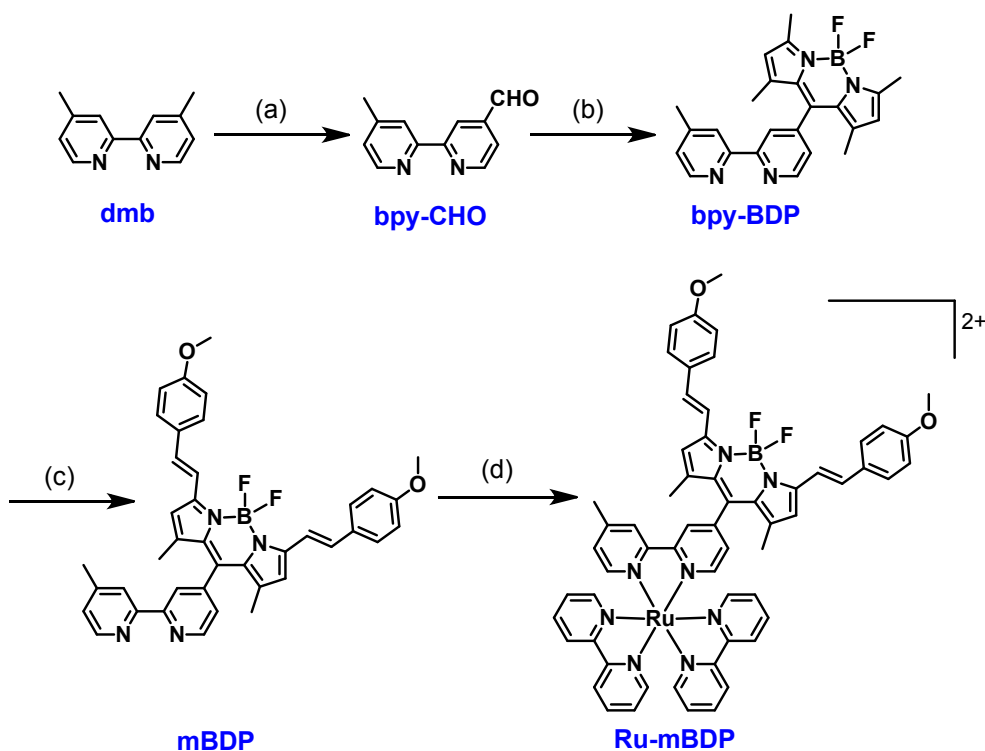
All reagents purchased from commercial sources were used without further purification. 2,2,6,6-tetramethylpiperidine (TEMP), 2,2,6,6-tetramethylpiperidine-1-oxyl (TEMPO), NaN_3 , $\text{BF}_3 \cdot \text{OEt}_2$, triethylamine (TEA), 2,4-dimethyl-1H-pyrrole, 2,3-dichloro-5,6-dicyano-p-benzoquinone (DDQ), 4,4'-dimethyl-2,2'-bipyridyl, cisplatin, 3-(4,5-dimethylthiazol-2-yl)-2,5-diphenyltetrazolium bromide (MTT) and 1,3-diphenyliso-benzofuran (DPBF) were purchased from Sigma-Aldrich. Chlorin e6 (Ce6) were purchased from J&K Scientific. Dulbecco's modified eagle medium (DMEM), fetal bovine serum (FBS), penicillin, streptomycin, LIVE/DEAD™ viability/cytotoxicity kit, LysoTracker Green DND-26, ER-Tracker™ Green and MitoTracker® Green FM were purchased from Thermo Fisher. The 2',7'-dichlorofluorescein diacetate (DCFH-DA), Hoechst 33342 and annexin V-FITC apoptosis detection kit were obtained from the Beyotime Biotechnology. Caspase-3/7 activity kit were purchased from Promega (USA). Acridine orange (AO) and Magic Red cathepsin B assay kit were purchased from ImmunoChemistry Technologies. The complexes were prepared in DMSO (10 mM) as stock solution and were stored in the dark, and aliquots of the stock solution were added to the cultured system to give a desired diluted concentration of the complex with a final DMSO content less than 1% throughout this study. Cisplatin stock solution (3 mM) were prepared in saline, stored in the dark and used within 1 week.

^1H NMR spectra were recorded on a 400 MHz Bruker Avance 300 spectrometer nuclear magnetic resonance spectrometer. Electrospray ionization mass spectra (ESI-MS) was recorded on an LTQ XL system (Thermo, USA). Analysis of elements (C, H, and N) was carried out using an Elemental Vario EL CHNS analyzer (Germany). The EPR spectra were measured using a Bruker e-scan EPR spectrometer. The electronic absorption spectra and emission spectra were recorded at room temperature using a Perkin-Elmer Lambda 850 UV/Vis spectrometer and Perkin-Elmer LS 55 luminescence spectrometer, respectively. Cell imaging experiments were implemented on an LSM 880 Zeiss laser scanning confocal microscope (CLSM) and Zeiss inverted fluorescence microscope. The inductively coupled plasma mass spectrometry (ICP-MS) experiments were performed using a Thermo Fisher's iCAP RQ instrument. Irradiation was provided by a commercially available LED area light source ($\lambda_{\text{irr}} = 660$ nm, 15.7 mW/cm², Height LED Instruments, China), Flow cytometry experiments were conducted on a BD FACS Canto II flow cytometer. Cell viability and caspase-3/7 activity experiments were conducted on a TECAN Infinite M200 PRO multifunctional reader. The in vivo fluorescence imaging experiment was carried out by an IVIS in vivo imaging system (PerkinElmer, Lumina XRMS Series III, USA).

Synthesis and characterization

4-methyl-2,2'-bipyridine-4'-carboxaldehyde (**bpy-CHO**) ^[1], 5,5-difluoro-1,3,7,9-

tetramethyl-10-(4'-methyl-[2,2'-bipyridin]-4-yl)-5H-dipyrrolo[1,2-c:2',1'-f][1,3,2]diazaborinin-4-ium-5-uide (**bpy-BDP**)^[1], Ru(bpy)₂Cl₂^[2] were obtained according to the previously published literature. [Ru(bpy)₂(dmb)]²⁺ (**Ru-dmb**, **dmb** = 4,4'-dimethyl-2,2'-bipyridine)^[3] and 5,5-difluoro-3,7-bis((E)-4-methoxystyryl)-1,9-dimethyl-10-(4'-methyl-[2,2'-bipyridin]-4-yl)-5H-dipyrrolo[1,2-c:2',1'-f][1,3,2]diazaborinin-4-ium-5-uide (**mBDP**)^[4,5] were synthesized based on modified methods of the literatures. Synthetic routes of **mBDP** and **Ru-mBDP** were shown in **Scheme S1**.



Scheme S1. Synthesis routes of **mBDP** and **Ru-mBDP**. (a) SeO₂, dioxane, reflux overnight. (b) 2,4-dimethylpyrrole, DCM, TFA, DDQ, TEA, BF₃·Et₂O. (c) 4-methoxybenzaldehyde, glacial acetic acid, piperidine (d) Ru(bpy)₂Cl₂, EtOH/H₂O, 80 °C, 12 h

Synthesis of **mBDP**

bpy-BDP (0.416g, 1 mmol) and 4-methoxybenzaldehyde (0.408 g, 3 mmol) were dissolved in a mixture of toluene (50 mL), glacial acetic acid (1 mL), and piperidine (1.2 mL), and were refluxed overnight in a Dean-Stark apparatus. The reaction was monitored by TCL (silica), and was ceased when the product leveled off. Crude product was concentrated under vacuum to a residue, and was dissolved in DCM, washed thrice by water. The organic layer was dried by anhydrous Na₂SO₄, evaporated under vacuum to give a crude product. Further purification by silica gel column chromatography (DCM/EtOAc, v/v = 30:1) gave 0.15 g powder of **mBDP**. Yield rate: 23%. Anal. Calcd. for C₄₀H₃₅BF₂N₄O₂: C 73.62%, H 5.41%, N 8.59%. Found: C 73.34%, H 5.65%, N 8.46%. ES-MS [m/z]: [M+H]⁺ 653.84. ¹H NMR (400 MHz, Chloroform-d) δ 8.84 (d, J = 4.8 Hz, 1H), 8.55 (d, J = 5.5 Hz, 2H), 8.34 (s, 1H), 7.64 (s, 1H), 7.60 (s, 3H), 7.58 (s,

2H), 7.37 (dd, J = 4.8, 1.5 Hz, 1H), 7.25 (s, 1H), 7.20 (d, J = 4.9 Hz, 2H), 6.93 (d, J = 8.7 Hz, 4H), 6.62 (s, 2H), 3.86 (s, 6H), 2.49 (s, 3H), 1.52 (s, 6H).

Synthesis of **Ru-mBDP**

mBDP (0.130 g, 0.2 mmol) and Ru(bpy)₂Cl₂ (0.121 g, 0.22mol) were dissolved in 28 mL DCM/EtOH/H₂O (v/v/v = 3:10:1,) refluxed at 80 °C under argon atmosphere and protected from light. The reaction process was monitored by TLC (silica). Upon completion (i.e., exhaustion of **mBDP** in TLC), the solvent was removed under vacuum. The crude product was purified by column chromatography on alumina (MeCN/MeOH, v/v = 25:1) to give a black green solid. Yield: 0.107 g, 47%. Anal. Calcd. for C₆₀H₅₁BCl₂F₂N₈O₂Ru: C 63.39%, H 4.52%, N 9.86%. Found: C 63.22%, H 4.73%, N 9.73%. ES-MS [m/z]: [M-Cl₂]²⁺ 533.63. ¹H NMR (400 MHz, DMSO-d₆) δ 9.06 (s, 1H), 8.95 – 8.87 (m, 5H), 8.25 – 8.20 (m, 3H), 8.17 (dd, J = 9.9, 1.9 Hz, 1H), 7.92 – 7.86 (m, 3H), 7.78 (d, J = 5.2 Hz, 1H), 7.73 – 7.69 (m, 2H), 7.57 (dt, J = 12.0, 7.3 Hz, 11H), 7.40 (dd, J = 17.1, 11.8 Hz, 3H), 7.09 (s, 1H), 7.06 (dd, J = 8.8, 3.5 Hz, 4H), 6.94 (s, 1H), 3.83 (d, J = 1.7 Hz, 6H), 2.47 (s, 3H), 1.77 (s, 3H), 0.89 (s, 3H).

Synthesis of **Ru-dmb**

Ru(bpy)₂Cl₂ (0.097 g, 0.2 mmol) was mixed with equivalent **dmb** (0.037 g, 0.2 mmol) in EtOH/H₂O (v/v = 2:1), and refluxed overnight under argon and protected from light. The removal of the solution gave brown crude product which was further purified by column chromatography on alumina to give red powder. Yield: 0.097 g, 53%. Anal. Calcd. for C₃₂H₂₈Cl₂N₆Ru: C 57.49%, H 4.22%, N 12.57%. Found: C 57.33%, H 4.35%, N 12.48%. ES-MS [m/z]: [M-Cl₂]²⁺ 298.5. ¹H NMR (400 MHz, DMSO-d₆) δ 8.86 (d, J = 8.1 Hz, 4H), 8.76 (s, 2H), 8.16 (t, J = 7.9 Hz, 4H), 7.73 (t, J = 5.4 Hz, 4H), 7.56 – 7.50 (m, 6H), 7.37 (d, J = 5.1 Hz, 2H), 2.52 (s, 6H).

Electron paramagnetic resonance (EPR) assay

The EPR measurements were carried out with a Bruker Model A300 spectrometer at 298 K. A light irradiation system consisting of a 450 W xenon lamp and optical gratings was used to emit light above 400 nm. All EPR measurements were carried out by the following parameter settings to detect the spin adducts: 20 mW microwave power, 180 G-scan range, 100 G-scan range, and 1 G field modulation. The spin trap TEMP for trapping ¹O₂ (75 mM) was used to verify the formation of reactive oxygen species (ROS) generated by **BmBDP**, **Ru-dmb** and **Ru-mBDP** (25 μM). NaN₃ (100 mM) was used as ¹O₂ scavenger, and was further mixed with the indicated compounds before irradiation. All samples were evenly mixed with the spin trap, respectively, in capillary tubes and put into the EPR cavity. The EPR signals after various irradiation periods (0, 3 min) were recorded.

¹O₂ quantum yield measurement

The singlet oxygen quantum yields (Φ_{Δ}) of **mBDP**, **Ru-dmb** and **Ru-mBDP** were measured by a reported method^[6]. DPBF was used as the singlet oxygen (¹O₂) scavenger on account of the linear relationship between its reduced absorbance at 418 nm and the generated ¹O₂. The respective OD_{660 nm} of **mBDP** and **Ru-mBDP**, and OD_{450 nm} of **Ru-dmb** was adjusted to 0.15. The adjusted indicated compounds were mixed with DPBF (50 μ M), respectively, in an air-saturated DMSO solution, subjected to LED light irradiation. 660 nm (for **mBDP** and **Ru-mBDP**) and 450 nm (for **Ru-dmb**) irradiation sources were used in this experiment. The optical intensity at 418 nm was recorded after every 2 s period of irradiation. The ¹O₂ quantum yields of the indicated complexes were calculated according to the following equation,

$$\Phi_{\Delta}^S = \Phi_{\Delta}^R \times (m^S \times F^R)/(m^R \times F^S) \quad (1)$$

where the superscript 'R' stands for the reference compound (i.e., MB as reference for **Ru-mBDP**, $\Phi_{\Delta} = 0.49$; [Ru(bpy)₃]²⁺ as reference for **Ru-dmb**, $\Phi_{\Delta} = 0.66$ in DMSO);^[7] the superscript 'S' stands for the samples; m is the calibrated slope (by subtracting the absorption loss stemmed from photo-bleaching) of a linear fit of the cumulative absorption change at 418 nm vs. the irradiation time (s); F is the absorption correction factor, which is given by $F = 1 - 10^{-OD}$.

LogP_{O/W} measurement

The LogP_{O/W} value was measured by using a 'shake-flask' method. 50 mL n-octanol and 50 mL water were mixed and shaken at a sealed flask at R.T. for 48 h to yield n-octanol-saturated water and water-saturated n-octanol. These binary layers were separated and used in this experiment. **mBDP** n-octanol solution (5 μ M) and Ru(II) complex water solutions (10 μ M) were prepared using the above solvents. The solutions were then added with equal volume of the opposite-phase of solvent, and were vigorously shaken for another 48 h at R.T. to reach partition equilibrium of the indicated compounds between water and n-octanol. The binary layers were carefully divided for LogP_{O/W} analysis. The concentration of compounds in n-octanol phase (C_O) and water phase (C_W) were determined, respectively, using absorption spectrophotometry with the aid of a series of standard solutions. LogP_{O/W} values were calculated by the following equation,

$$\text{Log } P_{O/W} = \log(C_O/C_W) \quad (2)$$

Stability in aqueous environment

The stability of **Ru-mBDP** in aqueous environment was assessed by using a procedure analogous to a recently reported method. Diazepam (Sigma-Aldrich) solution was used as internal reference. For this experiment, 20 μ M **Ru-mBDP** and diazepam were added to the water to a total volume of 1 ml. The solution was shaken (~300 rpm) at 37 °C for 0 h and 48 h, respectively, and was then subjected to HPLC–UV analysis. A C8 reverse

phase column was used with an eluent flow rate of 0.5 mL/min. The runs were performed with a linear gradient of A (methyl alcohol, 0.1% TFA, v/v, Sigma-Aldrich HPLC grade) in B (distilled water, 0.1% TFA, v/v). The samples were eluted by using a program as follows: 60% B (0 min)--100% B (10 min)--100% B (20 min). The UV detector was set at 254 nm.

Cell line and culture conditions

All the cells were obtained from the Experimental Animal Centre of Sun Yat-Sen University (Guangzhou, China). A375, A549, HeLa, SGC7901, HepG2, and LO2 cell lines were cultured in Dulbecco's Modified Eagle's medium (DMEM, Gibco BRL) supplemented with 10% (v/v) fetal bovine serum (FBS, Gibco BRL), penicillin (100 units/mL) and streptomycin (50 units/mL) at 37 °C in a CO₂ incubator with a humidified atmosphere (95% air and 5% CO₂).

Cellular uptake assay

For cellular uptake studies, exponentially growing A375 cells were harvested and seeded onto 100 mm culture plates (Costar), and allowed to adhere for 24 h. The cells were incubated with refreshed medium with **Ru-mBDP** (1 μM) for different time periods (2 h, 4 h, 6 h, 8 h, and 12 h), respectively, at 37 °C in the dark. The cells were washed by PBS and detached with trypsin, collected and counted. The whole cell pellets were digested with 60% HNO₃ (500 μL) and 30% H₂O₂ (200 μL) at R.T. for 48 h. Then indium internal standard was added to the system and diluted with MilliQ water to obtain 2% HNO₃ sample solutions with 10 ppb indium internal standard. The Ru content was detected using a Thermo Fisher iCAP RQ instrument. Data were recorded as the mean ± standard deviation (n = 3).

The cellular uptake of **Ru-mBDP** (1 μM, 12 h) in A549, HeLa, SGC7901, HepG2, and LO2 cell lines were performed in the same way.

Cellular uptake comparison study: The cellular uptake comparison of **mBDP**, **Ru-dmb** and **Ru-mBDP** in A375 cells was made by CLSM imaging (1 μM, 4 h), and further temporal comparison of **Ru-dmb** and **Ru-mBDP** (1 μM) was made by ICP-MS experiment (6 h, 12 h). In CLSM imaging experiment, the excitation wavelength for **mBDP** and **Ru-mBDP** was set as 633 nm, and the emission signals were collected at 650 ± 20 nm and 680 ± 20 nm, respectively. The excitation wavelength for **Ru-dmb** was set as 450 nm, and the emission filters was 620 ± 20 nm.

Cellular uptake mechanism study

The cellular uptake mechanism of **Ru-mBDP** was studied by CLSM imaging. A375 cells were treated with various combinations of inhibitors with **Ru-mBDP**, then washed by PBS for three times prior to imaging. The excitation wavelength for **Ru-mBDP** was set as 633 nm, and the emission signals centered at 680 nm were collected. Details for the cellular treatment are shown as follows,

Temperature influence study: A375 cells were incubated with **Ru-mBDP** (1 μ M) for 2 h at 37 °C and 4 °C in dark, respectively.

Metabolic inhibition study: A375 cells were pretreated with 2-deoxy-D-glucose (50 mM) and oligomycin (5 μ M) for 1 h at 37 °C, and then exposed to **Ru-mBDP** (1 μ M) for 2 h at 37 °C in the dark.

Endocytic inhibition study: A375 cells were pretreated with chloroquine (50 μ M) or NH₄Cl (50 mM) for 30 min at 37 °C, and then exposed to **Ru-mBDP** (1 μ M) for 2 h at 37 °C in the dark.

Cation translocator inhibition study: A375 cells were pretreated with tetraethylammonium (1 mM) for 30 min at 37 °C, and then exposed to **Ru-mBDP** (1 μ M) for 2 h at 37 °C in the dark.

Intracellular localization

The intracellular localization was studied by CLSM. A375 cells were adhered onto 35 mm Corning confocal dishes for 24 h, and treated with fresh medium with **Ru-mBDP** (1 μ M) at 37 °C for 4 h. Upon completion, cells were washed with PBS for three times, and exposed to DMEM with MitoTracker® Green FM (MTG, 150 nM), Lysotracker Green DND-26 (LTG, 150 nM), ER-Tracker™ Green (ERTG, 150 nM), and Hoechst 33342 (10 μ g/mL), respectively, for 0.5 h at 37 °C. Cells were then washed with PBS three times and imaged by CLSM under a 63 \times oil-immersion objective lens. The excitation wavelength for the Ru complex was set as 633nm, and 488 nm for MTG, LTG, and ERTG, and 405 nm for Hoechst 33342. Emission filters were set as follows: 680 \pm 20 nm (**Ru-mBDP**), 515 \pm 20 nm (MTG), 510 \pm 20 nm (LTG, ERTG), and 460 \pm 20 nm (Hoechst 33342).

Intracellular ROS generation

The intracellular reactive oxygen species (ROS) under irradiation were detected using the ROS probe, DCFH-DA. Exponentially grown A375 cells were seeded in 6-well plates, followed by 24 h incubation for attachment. A375 cells were preloaded with DCFH-DA (10 μ M) following the manufacture's protocols, then treated with culture medium (control), and different concentrations of **Ru-mBDP**, respectively, at 37 °C for 12 h in the dark. Upon completion, the culture medium was refreshed. The irradiation group cells were irradiated at 660 nm (0.5 J/cm²) while the dark group remained in the dark. Cells were collected and analyzed by flow cytometry (BD FACS CantoII).

Lysosomal membrane permeabilization analysis

AO was utilized to indicate lysosomal membrane permeabilization (LMP). A375 cells were seeded onto confocal dishes and treated with culture medium (control) and **Ru-mBDP** (0.025, 0.05 μ M), respectively, at 37 °C for 12 h in the dark. Upon completion, the culture medium was refreshed. The irradiation group cells were irradiated at 660 nm (0.5 J/cm²) while the dark group remained in the dark. Before imaging, the cells

were stained with AO (5 μM , 15 min), and imaged by CLSM. The filters were set as follows: i) green channel: $\lambda_{\text{ex}} = 488 \text{ nm}/\lambda_{\text{em}} = 505\text{-}545 \text{ nm}$; ii) red channel: $\lambda_{\text{ex}} = 488 \text{ nm}/\lambda_{\text{em}} = 610\text{-}640 \text{ nm}$.

Detection of cathepsin B release

A375 cells were seeded onto confocal dishes and treated with culture medium (control) and **Ru-mBDP** (0.025, 0.05 μM), respectively, at 37 °C for 12 h in the dark. Upon completion, the culture medium was refreshed. The irradiation group cells were irradiated at 660 nm (0.5 J/cm²) while the dark group remained in the dark. Before imaging the cells were stained with cathepsin B fluorogenic substrate Magic Red MR-(RR)₂ for 1 h following the manufacture's protocols. The cells were imaged using CLSM with the excitation wavelength of 561 nm, and emission wavelength of 630 \pm 20 nm.

Caspase-3/7 activity assay

A375 cells were seeded on white-walled nontransparent-bottomed 96-well plates and treated with different concentrations of **Ru-mBDP**, and cisplatin, respectively, for 12 h in the dark. Then cells of the irradiation group were irradiated at 660 nm (0.5 J/cm²) while cells of the dark group remained in the dark. Both groups were further incubated for 12 h. Then the caspase-3/7 activity was measured according to the protocol of Caspase Glo[®] 3/7 Assay kit, and the luminescence was quantified by a TECAN micro plate reader.

Annexin V-FITC/PI staining assay

Exponentially grown A375 cells were seeded in 6-well plates, followed by 24 h incubation for attachment. After culture medium refreshing, cells were treated with culture medium, cisplatin, and different concentrations of **Ru-mBDP**, respectively, and incubated for 12 h at 37 °C in the dark. Upon completion, the culture medium was refreshed. The irradiation group cells were irradiated at 660 nm (0.5 J/cm²) while the dark group remained in the dark. Cells were further incubated 12 h then collected and stained with annexin V-FITC and propidium iodide (PI) following the manufacture's protocols. The results were obtained by flow cytometry.

In vitro cell viability test (MTT assay)

The cell viability was determined by MTT assay using A375, A549, HeLa, SGC7901, HepG2 and LO2 cells. Exponentially grown cells were seeded in 96-well plates, followed by 24 h incubation for attachment. Cells were incubated with different concentrations of **Ru-mBDP** and **Ce6**. For phototoxicity studies, after 12 h incubation, supernatant was replaced with fresh culture medium and cells were subjected to irradiation (LED system 660 \pm 5 nm; 15.7 mW/cm², light dose = 0.5 J/cm²), and incubated for additional 32 h. Cells without irradiation were replaced with fresh culture

medium and maintained in the dark. Then MTT was added and incubated for 4 h. The liquid was moved off and 150 μ L DMSO was charged to each well to dissolve the purple formazan crystals. Absorbance at 492 nm was measured by TECAN microplate reader. Data were reported as the mean \pm standard deviation ($n = 3$). IC_{50} values were determined by plotting the percentage of viability versus concentration on a logarithmic graph.

In vivo fluorescence imaging experiment

A375 tumor-bearing mice were intratumorally injected with **Ru-mBDP** (0.25 mg/kg), and subjected to fluorescence imaging. The fluorescence images were captured at different post-injection time by an IVIS (Ex: 640 nm, Em: 680 nm).

NIR PDT in vivo

BALB/c female nude mice aged 6-8 weeks were purchased and bred following the protocols of the laboratory animal center. All animal operations were in accordance with institutional animal use and care regulations approved by the Experimental Animal Centre of Sun Yat-Sen University. 120 μ L (*ca.* 3×10^6 cells / mL) A375 cells suspension in the mixture of saline with 30% Matrigel (Corning) was subcutaneously injected into the hind legs of four mice. The growing tumors were cut into approximately 1 mm³ fragments and transplanted into the right buttock of 20 nude mice using trocar in a sterile environment. When the volume of the A375 xenograft tumors reached to 20 ~ 40 mm³, the mice were randomly allocated into four groups (5 mice for each group): group 1, saline injection only; group 2, **Ru-mBDP** (25 μ L, 0.2 mg/mL) injection only; group 3, saline injection and subsequent irradiation; group 4, **Ru-mBDP** (25 μ L, 0.2 mg/mL) injection and subsequent irradiation. For irradiation group, the mice were anaesthetized by 10% chloral aqueous solution (240 μ L/20 g mice) 4 h after intra-tumor injection. All mice received two courses of drug administration and the corresponding PDT therapeutic regimens in the first week. Then these mice were subjected to red-light irradiation centered at 640 nm from a xenon lamp equipped with red-light monochromator (75 mW/cm², 10 min). The body weight and tumor volume data were recorded every 2 days in the therapeutic regimen, and the volumes of tumor were calculated by $0.5 \times \text{Length} \times \text{Width}^2$. The relative tumor volume is calculated by V/V_0 (V is the tumor volume on the day when data were recorded, V_0 is the tumor volume on the day when treatment was started). After two weeks of therapy, the mice were sacrificed, and the tumors and primary organs (heart, liver, spleen, lung, kidney, brain, and intestine) were obtained for histological analysis by hematoxylin-eosin (H&E) staining. All sections were imaged by a Carl Zeiss Axio Imager Z2 microscope for the tissue structure and cell state of the sections.

All animal experiments were performed according to the Guide for the Care and Use of Laboratory Animals by the US National Institutes of Health (NIH Publication No. 85-23, revised in 2011). All animal experiments were reviewed and approved by the Institutional Animal Care and Use Committee (IACUC) at Sun Yat-Sen University,

Guangzhou, China (Approval No: IACUC-2017-09-21). We made every effort to minimize animal suffering and to reduce the number of animals used.

Supporting Figures

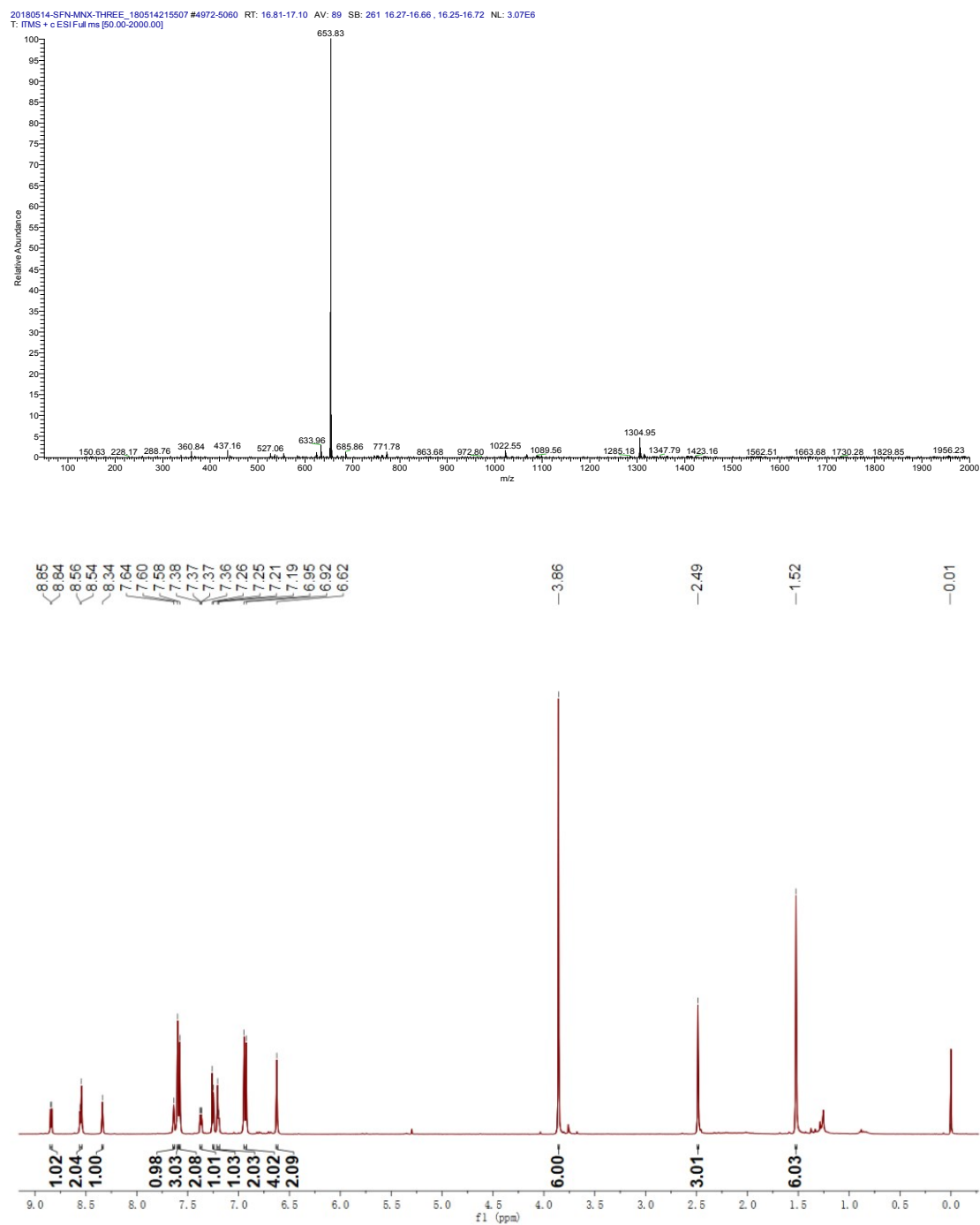


Fig. S1 ES-MS, and ¹H NMR spectra of **mBDP**

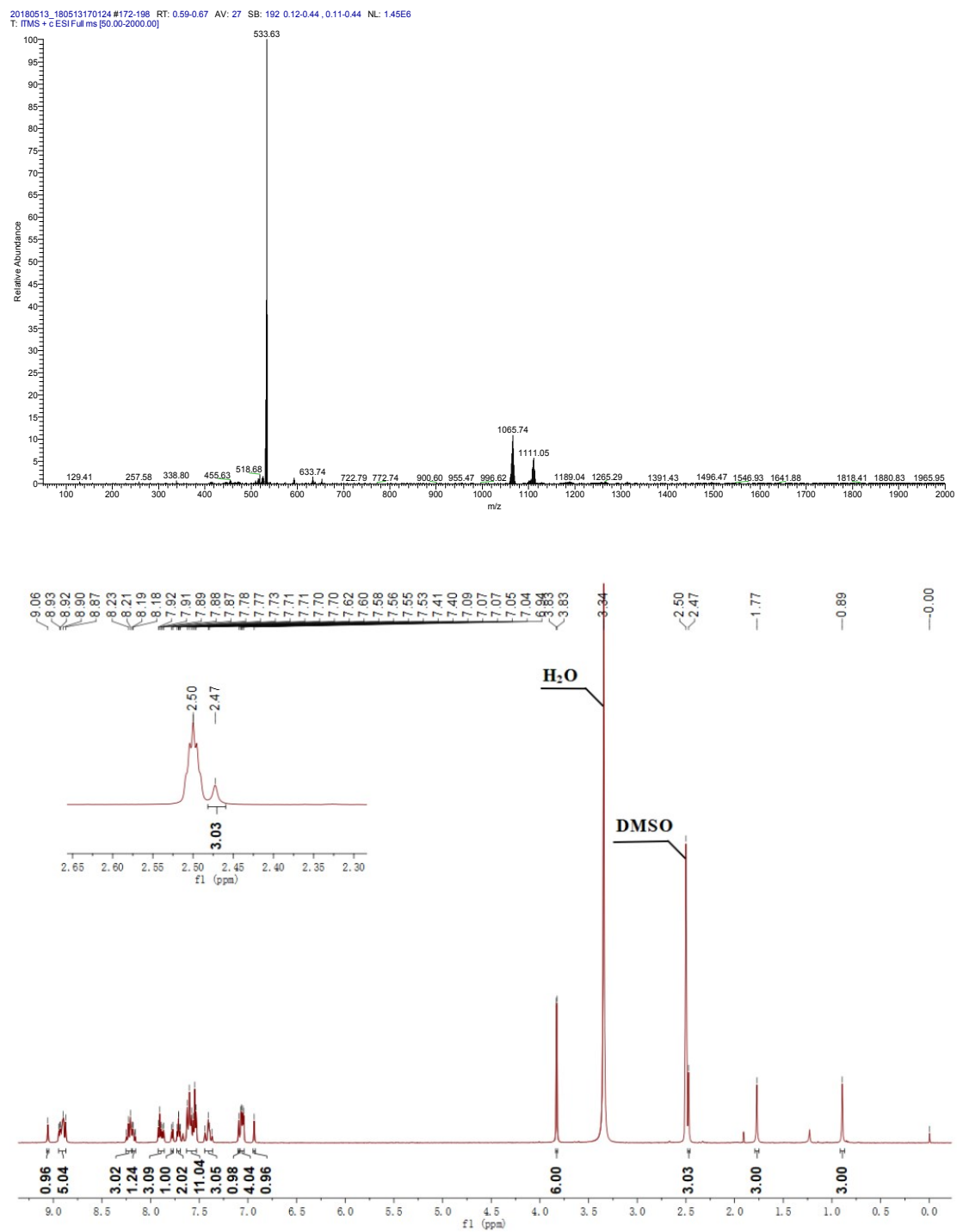


Fig. S2 ES-MS, and ¹H NMR spectra of **Ru-mBDP**

Peak#:1 Ret.Time:Averaged 1.367-1.400(Scan#:83-85)
BG Mode:Calc 1.317<->1.600(80<->97)
Mass Peaks:897 Base Peak:298.50(1687148) Polarity:Pos Segment1 - Event1

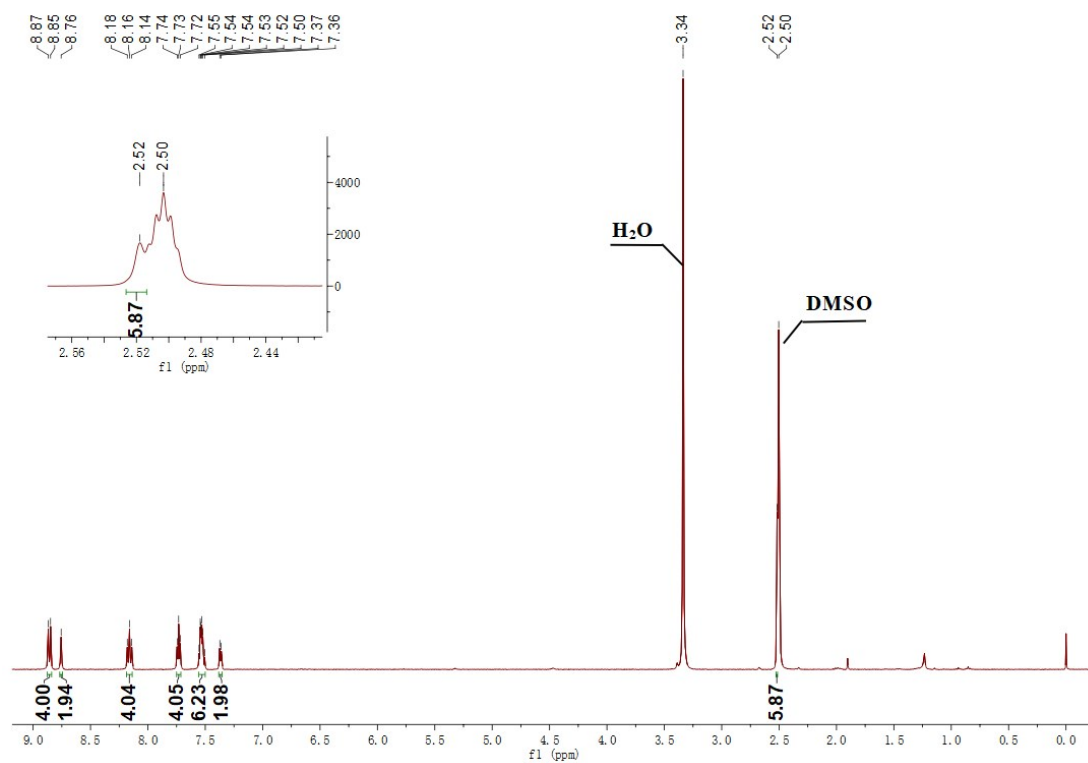
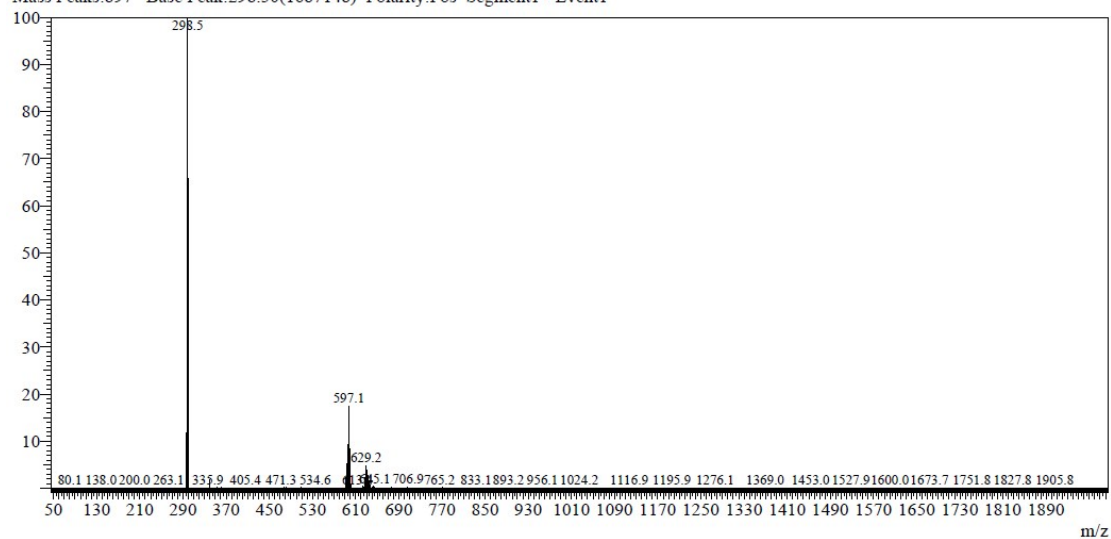


Fig. S3 ES-MS, and ^1H NMR spectra of Ru-dmb

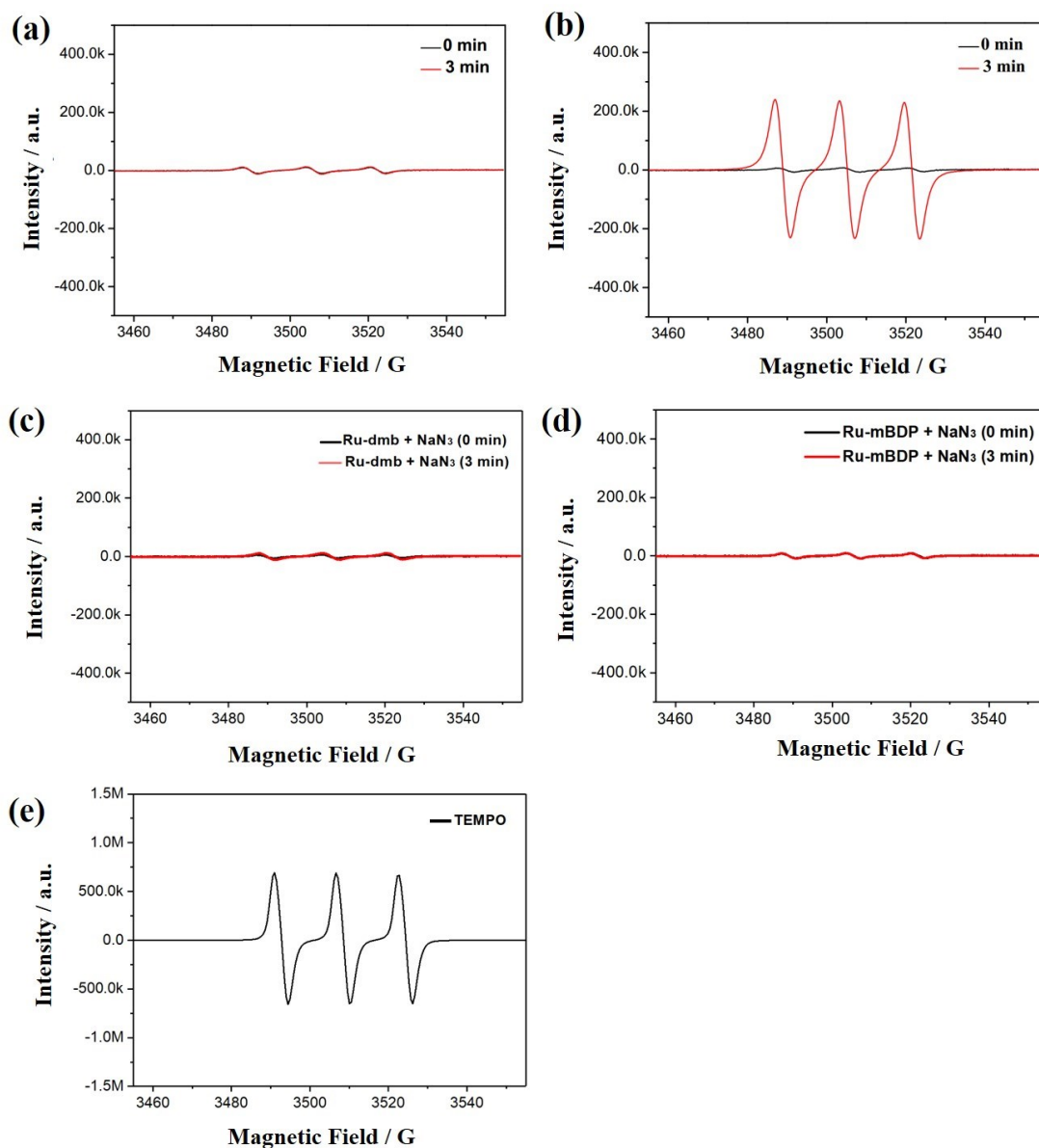


Fig. S4 EPR signals of **mBDP** (a), **Ru-dmb** (b), **Ru-dmb + NaN₃** (c), and **Ru-mBDP + NaN₃** (d), respectively, trapped by TEMP in DMSO in the presence of various irradiation periods. Irradiation wavelengths for **mBDP** and **Ru-mBDP** is 660 nm, and that for **Ru-dmb** is 450 nm. (e) The EPR signal of TEMPO (adduct of ¹O₂ with TEMP) was provided as a reference. NaN₃ (100 mM) was used as ¹O₂ scavenger.

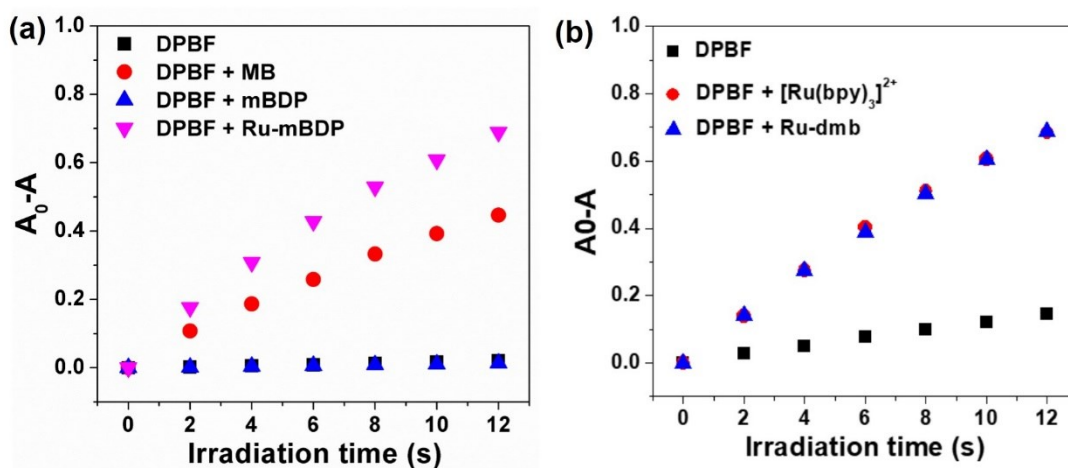


Fig. S5 Photooxidation of DPBF by **mBDP**, **Ru-dmb** and **Ru-mBDP** in aerated DMSO. Trajectory of optical intensity of DPBF at 418 nm when exposed to irradiation at 660 nm (a) and 450 nm (b). MB and [Ru(bpy)₃]²⁺ were used, respectively, as reference the compound for (a) and (b).

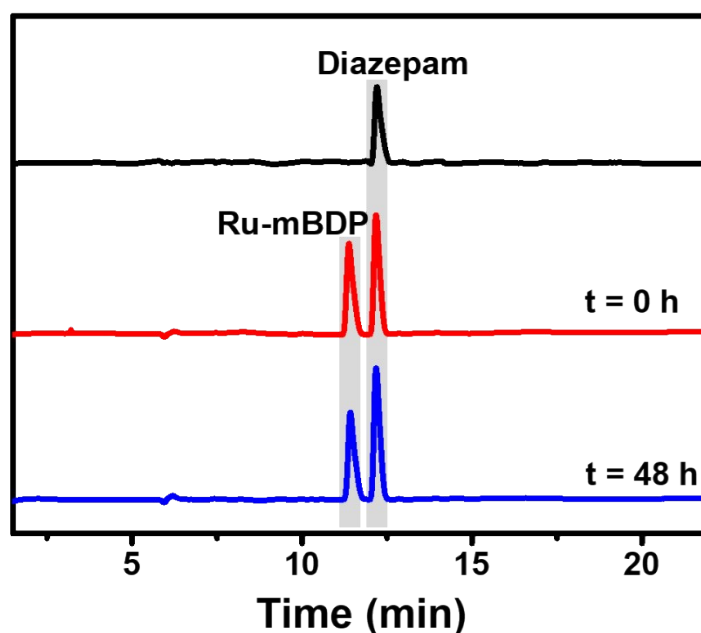


Fig. S6 The HPLC results for the stability of **Ru-mBDP** in H₂O containing 0.1% DMSO. Red line: fresh preparation; Blue line: solution stored at 37 °C for 48 h in the dark. Diazepam was used as internal standard. **Ru-mBDP** was mixed with diazepam and incubated in aqueous environment for 0 h and 48 h, respectively.

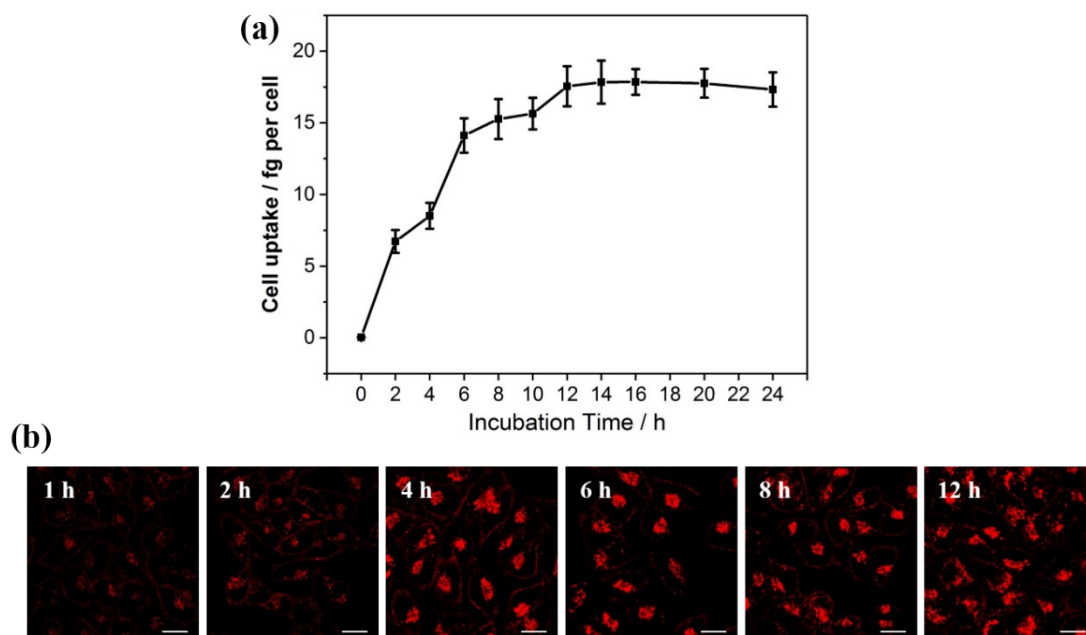


Fig. S7 Temporal profiles of a) ICP-MS analysis and b) confocal imaging analysis of cellular uptake of **Ru-mBDP** (1 μ M) in A375 cells.

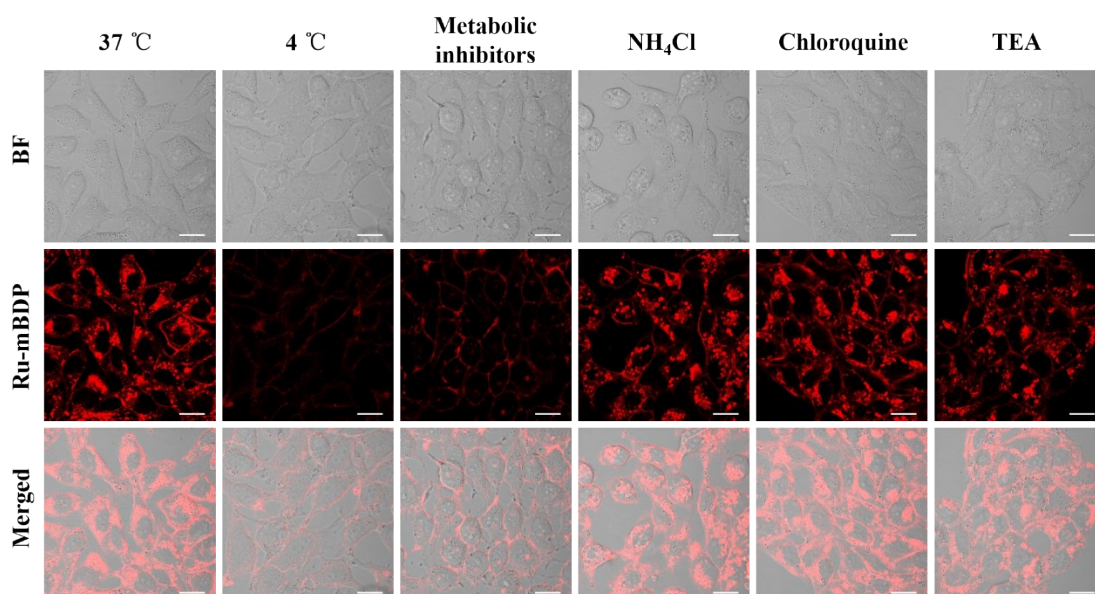


Fig. S8 Cellular uptake mechanism study of **Ru-mBDP** (1 μ M, 2 h) in A375 cells under different conditions. Scale bars represent 20 μ m.

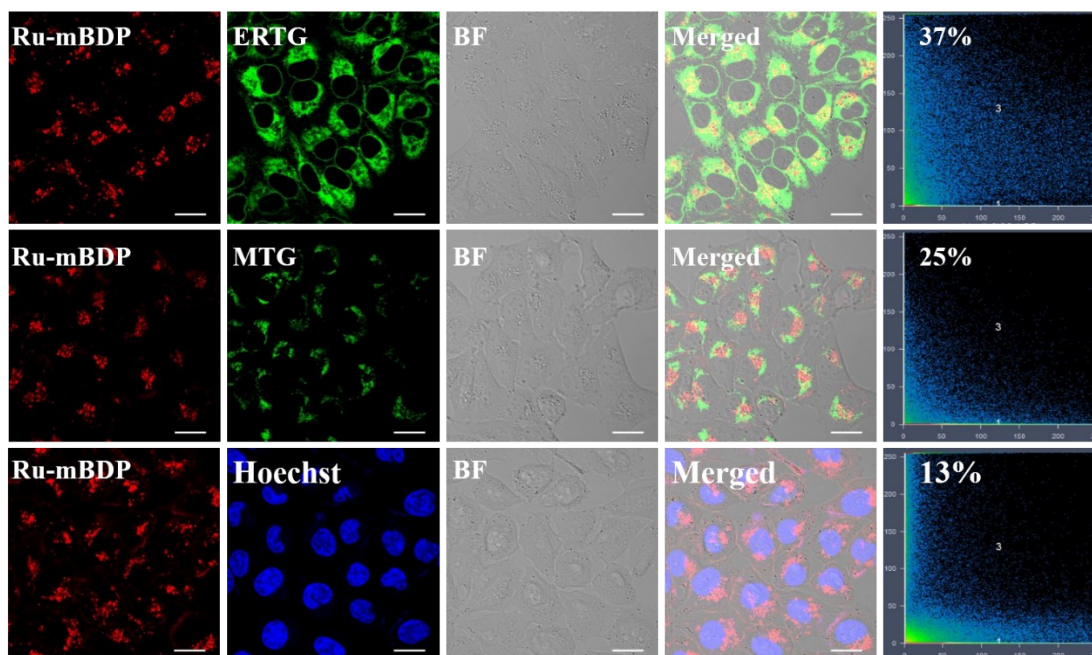


Fig. S9 Subcellular distribution confocal study of **Ru-mBDP** in A375 cells by co-localization imaging. Pearson's co-localization coefficients are provided in the rightmost column. The imaging parameters were set as follows: **Ru-mBDP** ($\lambda_{\text{ex}} = 633 \text{ nm}$, $\lambda_{\text{em}} = 680 \pm 20 \text{ nm}$), **MTG** ($\lambda_{\text{ex}} = 488 \text{ nm}$, $\lambda_{\text{em}} = 515 \pm 20 \text{ nm}$), **ERTG** ($\lambda_{\text{ex}} = 488 \text{ nm}$, $\lambda_{\text{em}} = 510 \pm 20 \text{ nm}$), and **Hoechst 33342** ($\lambda_{\text{ex}} = 405 \text{ nm}$, $\lambda_{\text{em}} = 460 \pm 20 \text{ nm}$). Inset scale bars represent $20 \mu\text{m}$.

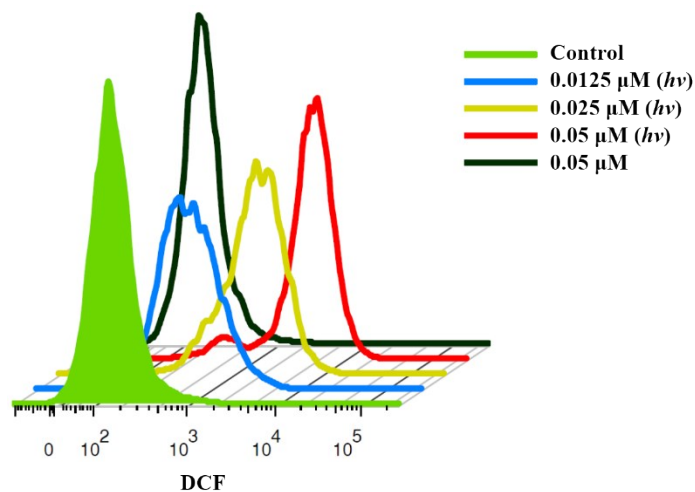


Fig. S10 ROS content measured with DCFH-DA in A375 cells treated with different concentrations of **Ru-mBDP** with or without irradiation (660 nm , 0.5 J/cm^2).

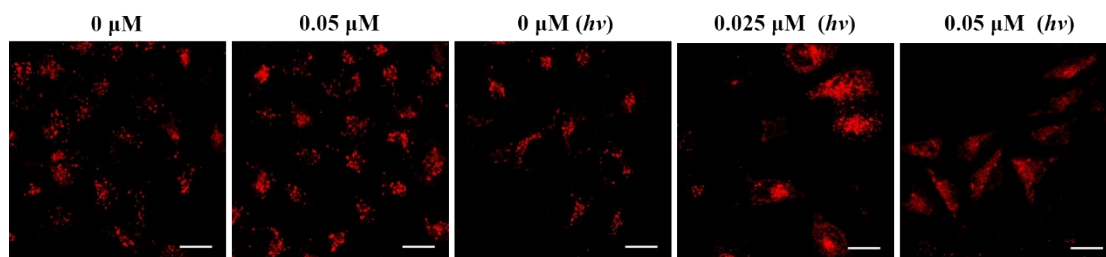


Fig. S11 Cathepsin B release from lysosomes to the cytosol in A375 cells treated with control and **Ru-mBDP** by fluorogenic substrate Magic Red MR-(RR)₂ assay with or without irradiation (660 nm, 0.5 J/cm²) (scale bar: 20 μm).

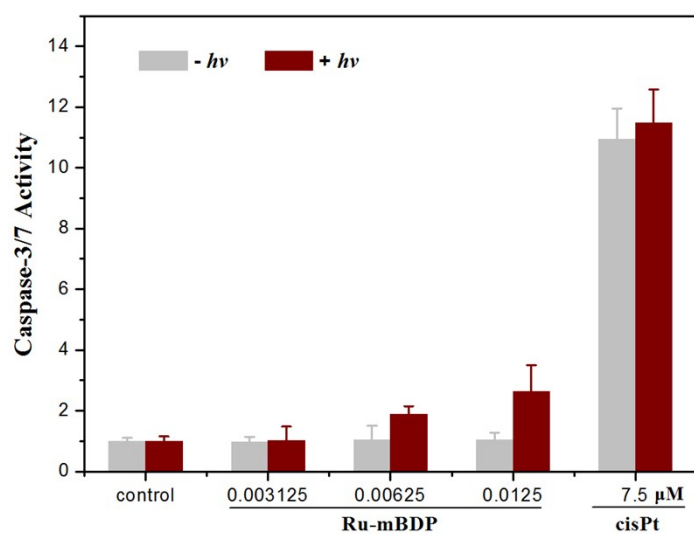


Fig. S12 Caspase-3/7 activity in A375 cells treated with different concentrations of **Ru-mBDP**, and cisplatin, respectively, in the absence and presence of irradiation ($\lambda_{irr} = 660$ nm, 0.5 J/cm²).

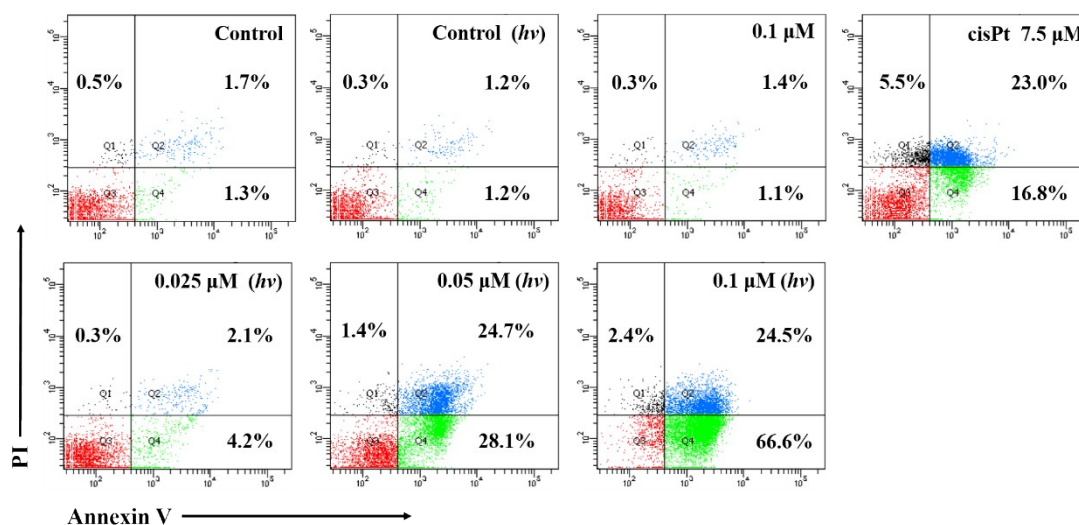


Fig. S13 Cell death examined by annexin V-FITC/PI co-staining assay. A375 cells were treated with culture medium, cisplatin, and different concentrations of **Ru-mBDP**, respectively, with or without irradiation ($\lambda_{\text{irr}} = 660 \text{ nm}$, 0.5 J/cm^2). The percentages of cells in each quadrant are annotated therein.

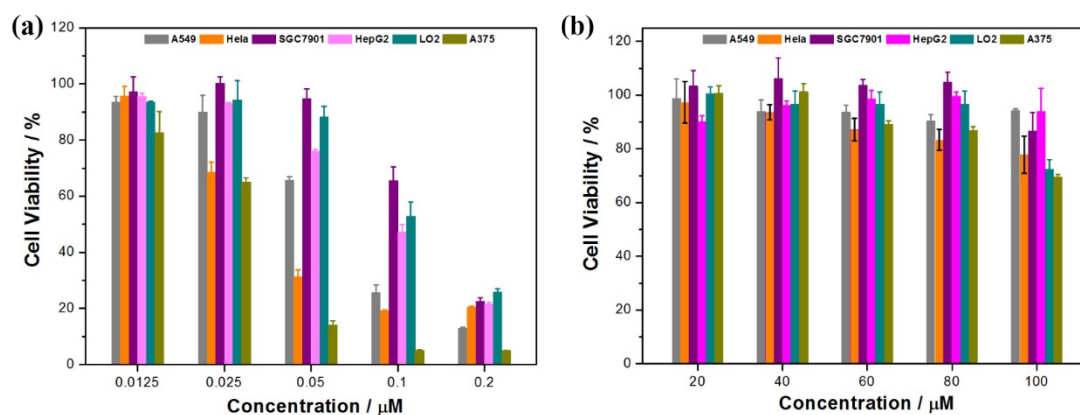


Fig. S14 Cell viability of different cells treated with different concentrations of **Ru-mBDP** with (a)/without (b) irradiation ($\lambda_{\text{irr}} = 660 \text{ nm}$, 0.5 J/cm^2).

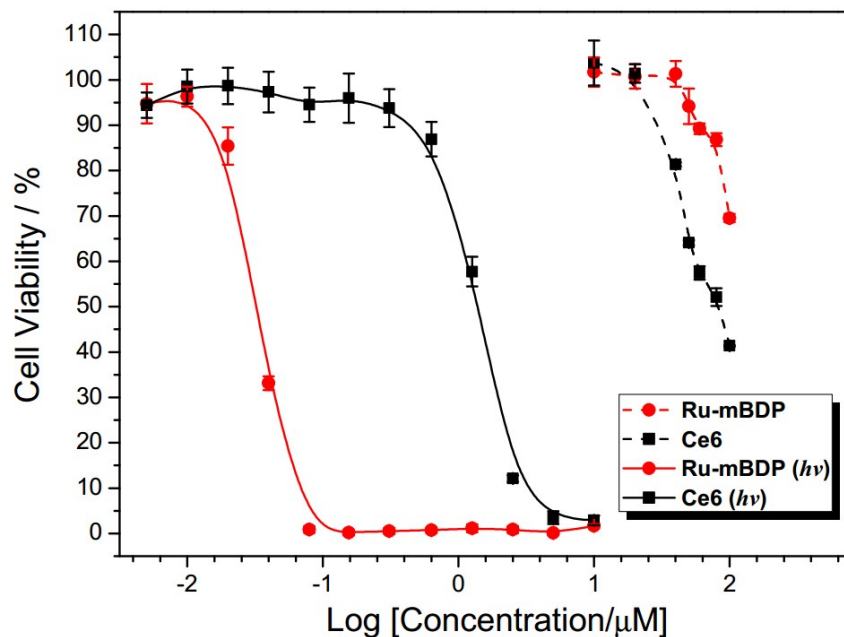


Fig. S15 The 48 h dosage-dependent PDT lethality study (by MTT) of **Ru-mBDP** in A375 in comparison with reference compound, **Ce6**, in the presence or absence of irradiation ($\lambda_{irr} = 660 \text{ nm}$, 0.5 J/cm^2).

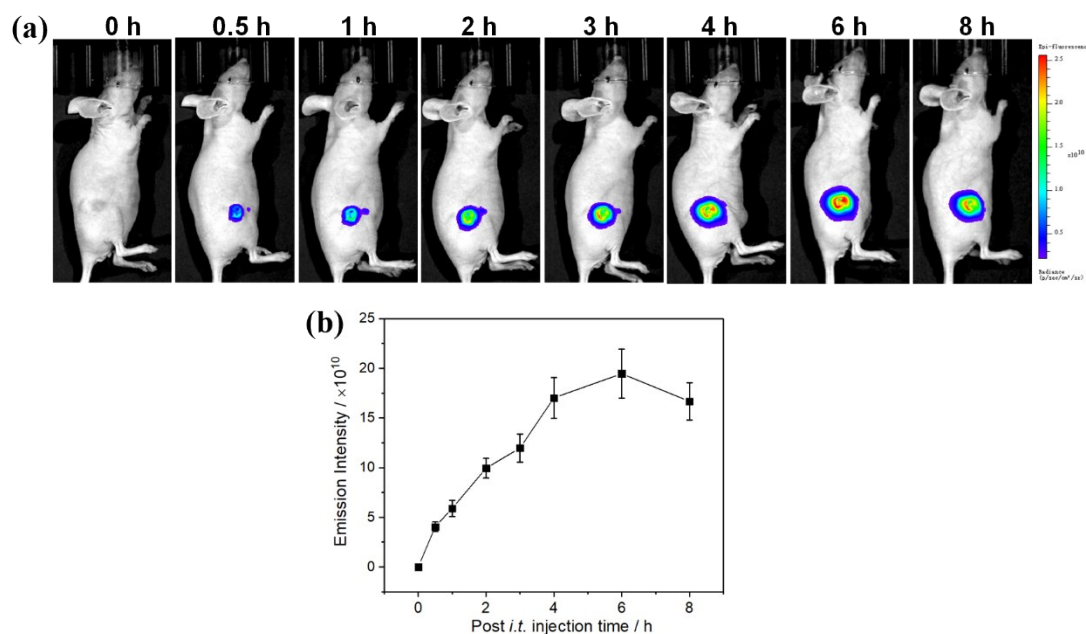


Fig. S16 In vivo post-injection temporal fluorescence imaging. (a) In vivo fluorescence images of A375 tumor-bearing nude mice taken at different time points post i.t. injection of **Ru-mBDP** (0.25 mg/kg). (b) Quantitative fluorescence signal intensities in tumor region.

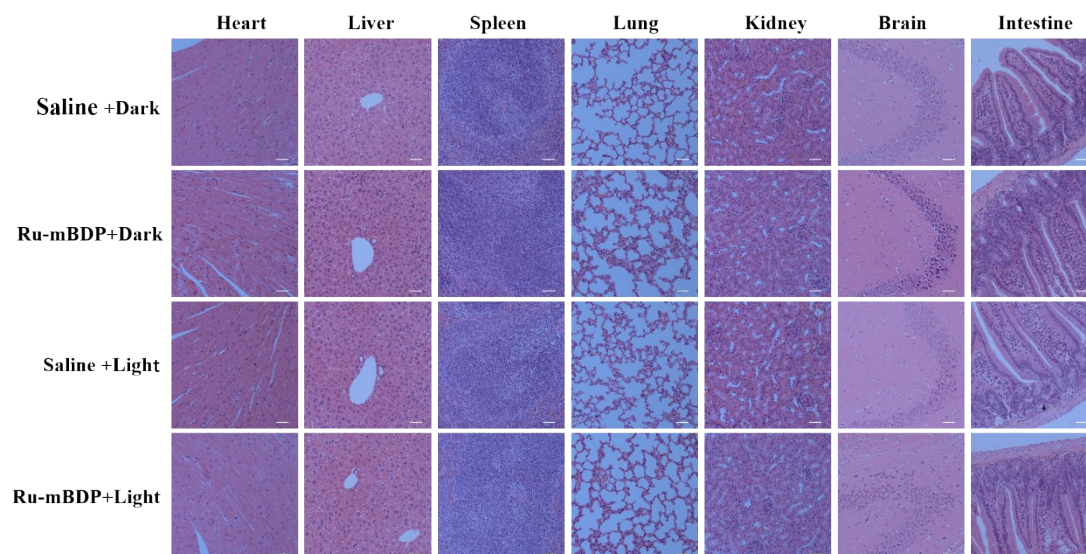


Fig. S17 H&E staining of tumor/organ slices from different groups (I, saline + dark; II, **Ru-mBDP** + dark; III, saline + irradiation; IV, **Ru-mBDP** + irradiation). Inset scale bars: 50 μ m.

Supporting Tables

Table S1. Photophysical properties of the complexes.^a

| Compound | $\lambda_{\text{abs}}^{\text{b/nm}}$ (log ϵ ^c) | $\lambda_{\text{em}}/\text{nm}$ | Φ (%) ^d | $\Phi_{\Delta}(^1\text{O}_2)^{\text{g}}$ |
|----------------|---|---------------------------------|-------------------------|--|
| mBDP | 372(4.83), 593(4.59), 641(5.04) | 657 | 77.5 ^e | 0 ^h |
| Ru-dmb | 286(4.87), 454(4.10) | 623 | 3.93 ^f | 0.66 ⁱ |
| Ru-mBDP | 287(4.98), 375(4.89), 452(4.49), 603(4.63), 652(5.08) | 681 | 27.5 ^e | 0.77 ^h |

^a Data recorded in MeCN solution (10 μM), 298 K.

^b λ_{abs} denotes the wavelength corresponding to absorption maximums.

^c Molar absorption coefficient at the absorption maxima ($\text{M}^{-1}\text{cm}^{-1}$).

^d Luminescent quantum yield.

^e Using ZnPc ($\Phi_{\text{L}} = 0.28$ in DMF) as the reference compound [5].

^f Using $[\text{Ru}(\text{bpy})_3]^{2+}$ ($\Phi_{\text{L}} = 0.063$ in DMF) as the reference compound [8].

^g Singlet oxygen quantum yield in DMSO

^h Using MB (0.49) as reference [7]

ⁱ Using $[\text{Ru}(\text{bpy})_3]^{2+}$ (0.66) as reference [7]

Table S2. 48 h (photo-)cytotoxicity profile in different cell lines (IC_{50} , μM).

| Cell line | A375 | | | A549 | | | HeLa | | |
|----------------------------|----------------|-------------------|-------|----------------|------------------|-------|----------------|-------------------|-------|
| | dark | light | PI | dark | light | PI | dark | light | PI |
| mBDP^a | >10 | >10 | - | >10 | >10 | - | >10 | >10 | - |
| Ru-dmb^b | >300 | >300 | - | >300 | >300 | - | >300 | >300 | - |
| Ru-mBDP^a | >100 | 0.029 \pm 0.004 | >3448 | >100 | 0.066 \pm 0.01 | >1515 | >100 | 0.049 \pm 0.005 | >2048 |
| Ce6 ^a | 79.1 \pm 2.0 | 1.3 \pm 0.8 | 61 | >100 | 7.8 \pm 0.9 | >13 | >100 | 11.4 \pm 1.1 | >9 |
| cisplatin ^a | 7.0 \pm 0.3 | 7.1 \pm 0.4 | 1.0 | 14.9 \pm 1.4 | 14.7 \pm 0.7 | 1.0 | 6.1 \pm 0.6 | 6.0 \pm 0.7 | 1.0 |
| cisplatin ^b | 8.3 \pm 0.3 | 7.3 \pm 1.0 | 1.1 | 11.4 \pm 1.1 | 10.5 \pm 0.9 | 1.1 | 6.8 \pm 0.8 | 6.8 \pm 0.6 | 1.0 |
| Cell line | SGC7901 | | | HepG2 | | | LO2 | | |
| | dark | light | PI | dark | light | PI | dark | light | PI |
| mBDP^a | >10 | >10 | - | >10 | >10 | - | >10 | >10 | - |
| Ru-dmb^b | >300 | >300 | - | >300 | >300 | - | >300 | >300 | - |
| Ru-mBDP^a | >100 | 0.14 \pm 0.03 | >714 | >100 | 0.11 \pm 0.04 | >909 | >100 | 0.12 \pm 0.02 | >833 |
| Ce6 ^a | >100 | 14.2 \pm 1.5 | >7 | >100 | 4.0 \pm 0.85 | >25 | >100 | 8.5 \pm 0.9 | >12 |
| cisplatin ^a | 11.5 \pm 1.2 | 12.3 \pm 1.7 | 0.93 | 13.5 \pm 0.9 | 13.1 \pm 0.9 | 1.0 | 11.2 \pm 0.9 | 11.4 \pm 1.2 | 0.98 |
| cisplatin ^b | 12.5 \pm 1.1 | 11.6 \pm 0.7 | 1.1 | 8.1 \pm 0.8 | 8.4 \pm 0.4 | 0.96 | 11.4 \pm 0.8 | 11.3 \pm 0.8 | 1.0 |

^a Compound irradiated at 660 nm by an LED area light (0.5 J/cm^2).

^b Compound irradiated at 450 nm by an LED area light (0.5 J/cm^2).

References

1. L. A. Juárez, A. Barba-Bon, A. M. Costero, R. Martínez-Mañez, F. Sancenón, M. Parra, P. Gaviña, M. C. Terencio and M. J. Alcaraz, *Chem. Eur. J.*, 2015, **21**, 15486-15490.
2. B. P. Sullivan, D. J. Salmon and T. J. Meyer, *Inorg. Chem.*, 1978, **17**, 3334-3341.
3. S. A. McFarland, F. S. Lee, K. A. W. Y. Cheng, F. L. Cozens and N. P. Schepp, *J. Am. Chem. Soc.*, 2005, **127**, 7065-7070.
4. Y. Zhao, X. Lv, Y. Liu, J. Liu, Y. Zhang, H. Shi and W. Guo, *J. Mater. Chem.*, 2012, **22**, 11475.
5. L. Huang, Z. Li, Y. Zhao, J. Yang, Y. Yang, A. I. Pendharkar, Y. Zhang, S. Kelmar, L. Chen, W. Wu, J. Zhao and G. Han, *Adv. Mater.*, 2017, **29**, 1604789.
6. S. P. Li, C. T. Lau, M. Louie, Y. Lam, S. H. Cheng and K. K. Lo, *Biomaterials.*, 2013, **34**, 7519-7532.
7. L. V. Lutkus, S. S. Rickenbach and T. M. McCormick, *J. Photoch. Photobio. A*, 2019, **378**, 131-135.
8. J. V. Caspar and T. J. Meyer, *J. Am. Chem. Soc.*, 1983, **105**, 5583-5590.